

Steffen Hein

DSC numerical solution of the Oberbeck-Boussinesq equations

Abstract Dual Scattering Channel schemes generalise JOHNS' TLM algorithm and replace the latter in situations where the transmission line picture of wave propagation fails. This is notoriously the case in applications to fluid dynamics, for instance. In this paper, a DSC numerical solution of the OBERBECK-BOUSSINESQ equations is presented, which approximate the NAVIER-STOKES equations for viscous quasi incompressible flow with moderate variation in temperature.

Keywords: Time domain methods, DSC schemes, fluid dynamics, CFD, NAVIER-STOKES equations, BOUSSINESQ approximation.

MSC-classes: 65C20, 65M06, 76D05

Westerham on April 30, 2005

1. Introduction

Crushing the continuum down into mesh cells is a queer, artificial exercise. There are yet natural ways of computing the fields in a cellular mesh, and so to mitigate the disaster. Imposing a cellular mesh is tantamount to locally enforcing cell-boundary duality upon space - and the DSC setup offers a natural way to handling such situations.

Dual Scattering Channel (DSC) schemes are characterized by a two-step cycle of iteration which alternately updates the computed fields within cells and on their interfaces. If the updating instructions are explicit, then a near-field interaction principle leads to the typical structure of the DSC algorithm, viz. to its scattering process interpretation. A pair of vectors which represent the same field within a cell and on its surface essentially constitutes a *scattering channel*. An equivalent definition can be given in terms of a pair of distributions that 'measure' the field within the cell and on one of its faces. In the *primal* DSC scheme, which is the Transmission Line Matrix (TLM) method along JOHNS' line [JoB], ports of transmission line links visualise these distributions (finite integrals, in this case).

DSC schemes and their relation to the TLM method [Ch, Tlm1-3, Re] have been conceptually studied and technically analysed in [He1]. They are unconditionally stable under quite general circumstances - made tangible

with the notion of α -passivity [He2], and they are especially suitable for handling boundary conditions, non-orthogonal mesh, or also for replacing a staggered grid, where sometimes otherwise need of that is.

In section 2, we first recapitulate some characteristic features of DSC schemes, which in extenso are treated in [He1], before we deal in section 3 with the OBERBECK - BOUSSINESQ approximation to the NAVIER-STOKES equations. The DSC model outlined should be considered a *prototype*, first of all. In fact, the BOUSSINESQ equations for viscous fluid flow, inspite of retaining the often predominant non-linear advective part of the NAVIER-STOKES momentum equations, can only claim limited range of validity, due to significant simplifications. The OBERBECK-BOUSSINESQ approach is, however, prototypical also in providing a basis for most turbulence models [ATP], many of which can be implemented following the lines of this paper.

The treated implementation with unstructured hexahedral mesh, outlined in section 4, has recently been coupled to SPINNER's Maxwell field solver, allowing so for computing conductive and convective heat transfer simultaneously with the electric and magnetic heat sources in a lossy Maxwell field. Besides the underlying ideas and simplifications that enter the OBERBECK-BOUSSINESQ approximation and its DSC translation, some numerical results are displayed to illustrate and validate the approach.

2. Elements of DSC schemes

In this section, we resume some typical features of DSC schemes, referring the technically interested reader always to the systematic exposition [He1].

Given a mesh cell, we think of a *port* as a vector valued distribution, associated to a cell face (with support, however, *not* necessarily confined to that face, cf. sect.4), which assigns a state vector $z^p = (p, Z)$ to a physical field Z , the latter represented by a smooth vector valued function in space-time. We also require that in the given cell a *nodal image* p^\sim of p exists, such that

$$(1) \quad (p^\sim, Z) = (p \circ \sigma, Z) = (p, Z \circ \sigma^{-1}),$$

for every Z (of class C^∞ , e.g.), where σ denotes the spatial translation $\sigma: \mathbb{R}^3 \rightarrow \mathbb{R}^3$ that shifts the geometrical node (centre of cell) onto the (centre of) the respective face, cf. Fig1.

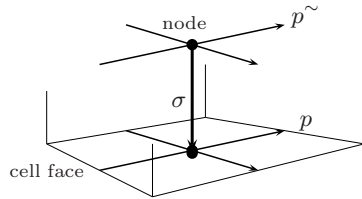


Fig. 1. Port on a cell face with nodal image.

DSC fields split thus into *port* and *node* components, z^p and z^n , which represent the field at the cell surfaces and within the cells. The two components are updated at even and odd integer multiples, respectively, of half a timestep τ and are usually constantly continued over the subsequent time intervals of length τ . Moreover, we assume that the updating instructions are *explicit*, i.e., with possibly time dependent functions F and G , for $t = m\tau$; $m \in \mathbb{N}$

$$(2) \quad \begin{aligned} z^n(t + \frac{\tau}{2}) &:= F([z^p]_t, [z^n]_{t-\frac{\tau}{2}}), \\ z^p(t + \tau) &:= G([z^p]_t, [z^n]_{t+\frac{\tau}{2}}), \end{aligned}$$

where $[z]_t$ stands for the entire sequence up to time t

$$[z]_t := (z(t - \mu\tau))_{\mu \in \mathbb{N}}$$

and we agree upon fixing $z^{p,n}(t) := 0$ for $t < 0$. (The 'back in time running' form of the sequence has certain technical advantages, cf. [He1].)

A fundamental DSC principle is *near-field interaction*, which spells that every updated state depends only on states (up to present time t) in the immediate neighbourhood. More precisely: The next nodal state depends only on states (with their history) in the same cell and on its boundary, and a subsequent port state depends only on states (again with history) on the same face and in the adjacent nodes.

As a consequence of near-field interaction, every DSC process allows for an interpretation as a multiple scattering process in the following sense.

If M is a mesh cell system and $\partial\zeta$ denotes the boundary of cell $\zeta \in M$, then every DSC state obviously permits a unique *scattering channel representation* in the space

$$P := \prod_{\zeta \in M} \prod_{p \in \partial\zeta} (z_\zeta^p, z_\zeta^{p^\sim}),$$

with canonical projections $\pi_\zeta^{p,n} : P \rightarrow P_\zeta^{p,n}$ into port and node components of cell ζ (the cell index is omitted, in general, if there is no danger of confusion). Also, there is a natural involutory isomorphism $nb : P \rightarrow P$

$$nb : (z^p, z^{p^\sim}) \mapsto (z^{p^\sim}, z^p),$$

which is named the *node-boundary map* and obviously maps P^p onto P^n and vice versa. For every DSC process $z = (z^p, z^n)(t)$, the following *incident* and *outgoing fields* z_{in}^p and z_{out}^n are then recursively well (viz. uniquely) defined, and are processes in P^p and P^n , respectively: For $t < 0$, $z_{in}^p(t) := z_{out}^n(t - \frac{\tau}{2}) := 0$, and for every $0 \leq t = m\tau$; $m \in \mathbb{N}$

$$(3) \quad \begin{aligned} z_{in}^p(t) &:= z^p(t) - nb \circ z_{out}^n(t - \frac{\tau}{2}), \\ z_{out}^n(t + \frac{\tau}{2}) &:= z^n(t + \frac{\tau}{2}) - nb \circ z_{in}^p(t). \end{aligned}$$

Hence, at every instant holds $z^p(t) = nb \circ z_{out}^n(t - \frac{\tau}{2}) + z_{in}^p(t)$ and $z^n(t + \frac{\tau}{2}) = nb \circ z_{in}^p(t) + z_{out}^n(t + \frac{\tau}{2})$. Then near-field interaction implies that every state is only a function of states incident (up to present time t) on scattering channels connected to the respective node or face. Precisely, it is shown that

Theorem 1 . *A pair of functions \mathcal{R} and \mathcal{C} exists, such that for every cell $\zeta \in M$ the process $z_\zeta^n = \pi_\zeta^n \circ z$ complies with*

$$(4) \quad z_\zeta^n(t + \frac{\tau}{2}) = \mathcal{R}((z_{in}^p(t - \mu\tau))_{p \in \partial\zeta; \mu \in \mathbb{N}})$$

and the port process $z_\zeta^p = \pi_\zeta^p \circ z$ satisfies

$$(5) \quad z_\zeta^p(t + \tau) = \mathcal{C}((z_{out}^n(t + \frac{\tau}{2} - \mu\tau))_{n| \partial\zeta; \mu \in \mathbb{N}}) .$$

(' | ' short-hand for 'adjacent to')

Remarks

- (i) The statements imply, of course, that $z_{\zeta, out}^n$ and $z_{\zeta, in}^p$ are themselves functions of states incident on connected scattering channels, since

$$(6) \quad \begin{aligned} z_{\zeta, out}^n(t + \frac{\tau}{2}) &= \mathcal{R}((z_{in}^p(t - \mu\tau))_{p \in \partial\zeta; \mu \in \mathbb{N}}) - z_{\zeta, in}^p(t) \quad \text{and} \\ z_{\zeta, in}^p(t) &= \mathcal{C}((z_{out}^n(t - \frac{\tau}{2} - \mu\tau))_{n| p; \mu \in \mathbb{N}}) - z_{\zeta, out}^{\sim}(t - \frac{\tau}{2}) \end{aligned}$$

- (ii) \mathcal{R} and \mathcal{C} are named the *reflection* and *connection* maps, respectively, of the DSC algorithm.
- (iii) Near field interaction is a constitutive element of computational stability, which is ensured, if the reflection and connection maps are *contractive* or *α -passive* [He2], in addition.

Proof. By induction and straightforward application of the *near-field interaction* principle. The statement is trivial for $t < 0$. If, for instance, (4) holds until $t - \frac{\tau}{2}$, then in virtue of (2) and remark (i) also

$$\begin{aligned} z_\zeta^n(t + \frac{\tau}{2}) &= F(\underbrace{[z_\zeta^p]_t}_{z_{\zeta, in}^p(t) + nb z_{\zeta, out}^n(t - \frac{\tau}{2})}, \underbrace{[z_\zeta^n]_{t - \frac{\tau}{2}}}_{\mathcal{R}[z_{\zeta, in}^p]_{t - \tau}}) \end{aligned}$$

is a function of states incident from $p \in \partial\zeta$ until t .

3. The dynamical equations

DSC algorithms are thus simply characterized as two-step explicit schemes that alternately update states in ports and nodes of a cellular mesh and which, in virtue of a near-field interaction principle, allow for a canonical interpretation as scattering processes. The latter exchange incident and reflected quantities between cells and their interfaces.

The ports and nodes are related to physical fields by vector valued distributions that evaluate the fields at cell faces and within the cells of a cellular mesh. Such a distribution may be a *finite integral*, as in the case of the TLM method, where finite path integrals over electric and magnetic fields are evaluated in a discrete approximation to Maxwell's integral equations [He3]. In the simplest case, it is only a *Dirac measure* that pointwise evaluates a field (or a field component) within a cell and on its surface. The distribution can also be a composite of Dirac measures that evaluate a field at different points in the cell - which applies, for instance, to the gradient functional treated in sect. 4.

Classical thermodynamics, with energy conservation in particular, entail the *convection-diffusion* equation for the temperature T in a fluid of velocity \mathbf{u} with constant thermal diffusivity α , heat source(s) q , and negligible viscous heat dissipation, viz.

$$(7) \quad \frac{\partial T}{\partial t} + \mathbf{u} \cdot \text{grad } T = \alpha \Delta T + q.$$

This is the energy equation for *Boussinesq-incompressible* fluids, e.g. [GDN]. The Navier-Stokes *momentum equations* for a fluid of dynamic viscosity μ , under pressure p , and in a gravitation field of acceleration \mathbf{g} require

$$(8) \quad \frac{\partial}{\partial t}(\varrho \mathbf{u}) + (\mathbf{u} \cdot \text{grad})(\varrho \mathbf{u}) + \text{grad } p = \mu \Delta \mathbf{u} + \varrho \mathbf{g}.$$

The *Oberbeck-Boussinesq* approximation [Obb],[Bss] starts from the assumption that the fluid properties are constant, except fluid density, which only in the gravitational term varies linearly with temperature; and that viscous dissipation can be neglected. Equations (8) become so with $\varrho_\infty = \text{const}$ and $\varrho(T) = \varrho_\infty \beta(T(t, \mathbf{x}) - T_\infty)$; $\beta := -\varrho^{-1} \partial \varrho / \partial T$

$$(9) \quad \frac{\partial \mathbf{u}}{\partial t} + (\mathbf{u} \cdot \text{grad}) \mathbf{u} + \frac{\text{grad } p}{\varrho_\infty} = \frac{\mu}{\varrho_\infty} \Delta \mathbf{u} + \beta(T(t, \mathbf{x}) - T_\infty) \mathbf{g}.$$

With the Gauss-Ostrogradski theorem applied to the integrals over $\Delta = \text{div grad}$ on cell ζ with boundary $\partial\zeta$, equations (7, 9) yield, with a time increment τ , the following updating instructions for T and \mathbf{u} averaged over the cell volume V_ζ

$$(10) \quad T(t + \frac{\tau}{2}) := T + \tau \{ -\mathbf{u} \cdot \text{grad } T + \frac{\alpha}{V_\zeta} \int_{\partial\zeta} \text{grad } T \cdot d\mathbf{F} + q V_\zeta \}$$

and

$$(11) \quad \begin{aligned} \mathbf{u}(t + \frac{\tau}{2}) &:= \mathbf{u} - \tau \{ (\mathbf{u} \cdot \text{grad}) \mathbf{u} + \frac{\text{grad} p}{\varrho_\infty} \} + \\ &+ \tau \{ \frac{\mu}{V_\zeta \varrho_\infty} \int_{\partial \zeta} \text{grad} \mathbf{u} \cdot d\mathbf{F} + \beta (T - T_\infty) \mathbf{g} \}. \end{aligned}$$

At the right-hand sides enter, of course, the last former updates (at time $t - \tau/2$ and t , respectively) of the nodal and cell face quantities.

T and \mathbf{u} so are updated at the reflection step of the DSC algorithm. In contrast, the cell surface integrals at the right-hand sides, in particular the gradients that enter these, are updated on the connection step.

The next section proceeds with that in unstructured hexahedral mesh.

4. The non-orthogonal hexahedral cell

The physical interpretation of a DSC algorithm associates a smoothly varying, i.e. in time and space sufficiently often continuously differentiable (for instance, C^∞) scalar or vector field Z to port and node states z^p and z^n of a mesh cell system.

For notational economy (so avoiding many ' \sum 's) in the following we adopt EINSTEIN's convention to sum up over identical right-hand sub and superscripts within terms where such are present, while summation is *not* carried out whenever a sub or superscript also appears somewhere as a left-hand index (for instance, in $(-1)^\kappa a_\kappa^\lambda b_\lambda c$ the sum is made over λ but not over κ).

Let a hexahedral cell be given by its eight vertices. Define then *edge vectors* $(_\nu e)_{\nu=0,\dots,11}$, *node vectors* $(_\mu b)_{\mu=0,1,2}$, and *face vectors* $(_\iota f)_{\iota=0,\dots,5}$, using the labelling scheme of figure 2 a

$$(12) \quad \begin{aligned} _\mu b &:= \frac{1}{4} \sum_{\nu=0}^3 (_{4\mu+\nu} e) & \mu = 0, 1, 2 \\ \text{and } _\iota f &:= \frac{(-1)^\iota}{4} ((_{8+2\iota} e + _{9+2(\iota+(-1)^\iota)} e) \wedge \\ &\quad \wedge (_{(4+2\iota)} e + _{(5+2\iota)} e)) & \iota = 0, \dots, 5, \end{aligned}$$

with all indices understood cyclic modulo 12 and \wedge denoting the cross product in \mathbb{R}^3 .

At every cell face $\iota \in \{0, \dots, 5\}$ and for any given $\tau \in \mathbb{R}_+$ the following time shifted finite differences of Z in directions $_\mu b$ ($\mu = 0, 1, 2$) form a vector valued function

$$(13) \quad _\iota \nabla^B Z_\mu(t) := \begin{cases} 2(-1)^\iota (Z^n|_{t-\tau/2} - _\iota Z^p|_t) & \text{if } \mu = [\iota/2] \\ (_{2\mu+1} Z^p - _{2\mu} Z^p)|_{t-\tau} & \text{if } \mu \neq [\iota/2] \end{cases}$$

($[x]$ denotes the *integer part* of $x \in \mathbb{R}$). The time increments are chosen conform with the updating conventions of DSC schemes (as will be seen in

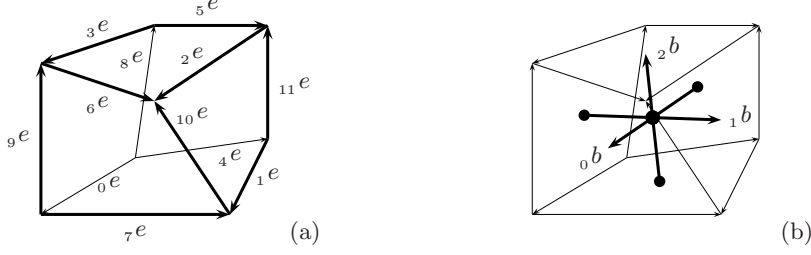


Fig. 2. Non-orthogonal hexahedral mesh cell.
(a) Edge vectors. (b) Node vectors.

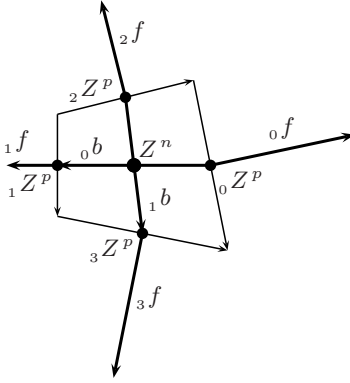


Fig. 3. Face vectors and port locations (nodal section).

a jiffy) and are consistent. In fact, in the first order of the time increment τ and of the linear cell extension, the vector ${}_{\iota}\nabla^B Z$ in the centre point of face ι approximates the scalar products of the node vectors with the gradient ∇Z . Let, precisely, for a fixed centre point on face ι and $\epsilon \in \mathbb{R}_+$ the ϵ -scaled cell have edge vectors ${}_{\iota}e^{\sim} := \epsilon {}_{\iota}e$. Let also ${}_{\iota}\nabla^{B^{\sim}} Z_{\mu}$ denote function (13) for the ϵ -scaled cell (with node vectors ${}_{\mu}b^{\sim} = \epsilon {}_{\mu}b$). Then at the fixed point holds

$$(14) \quad \langle {}_{\mu}b, \text{grad}(Z) \rangle = {}_{\mu}b \cdot \nabla Z = \lim_{\epsilon \rightarrow 0} \lim_{\tau \rightarrow 0} \frac{1}{\epsilon} {}_{\iota}\nabla^{B^{\sim}} Z_{\mu},$$

as immediately follows from the required C^1 -smoothness of the field Z .

To recover the gradient ∇Z from (13) in the same order of approximation, observe that for every orthonormal basis $({}_{\nu}u)_{\nu=0,\dots,m-1}$ of \mathbb{R}^m or \mathbb{C}^m , and for any basis $({}_{\mu}b)_{\mu=0,\dots,m-1}$ with coordinate matrix $\beta_{\nu}^{\mu} = \langle {}_{\nu}u, {}_{\mu}b \rangle$,

the scalar products of every vector a with ${}_\mu b$ equal

$$(15) \quad \underbrace{\langle {}_\mu b, a \rangle}_{=: \alpha_\mu^B} = \sum_{\nu=0}^{m-1} \underbrace{\langle {}_\mu b, {}_\nu u \rangle}_{(\bar{\beta}_\nu^\mu) = (\beta_\nu^\mu)^*} \underbrace{\langle {}_\nu u, a \rangle}_{=: \alpha_\nu} = \bar{\beta}_\mu^\nu \alpha_\nu$$

(at the right-hand side - and henceforth - observe EINSTEIN's convention), hence

$$(16) \quad \alpha_\nu = \gamma_\nu^\mu \alpha_\mu^B, \quad \text{with} \quad (\gamma_\nu^\mu) := ((\beta_\nu^\mu)^*)^{-1}.$$

In words: The scalar products of any vector with the basis vectors ${}_\mu b$ transform into the coordinates of that vector with respect to an orthonormal basis ${}_\nu u$ by multiplication with matrix $\gamma = (\beta^*)^{-1}$, where $\beta_\nu^\mu = \langle {}_\nu u, {}_\mu b \rangle$, i.e. β is the matrix of the coordinate (column) vectors ${}_\mu b$ with respect to the given ON-basis ${}_\nu u$, and γ its adjoint inverse.

This applied to the node vector basis ${}_\mu b$ and (14) yields the approximate gradient of Z at face ι

$$(17) \quad \iota \nabla Z_\nu = \gamma_\nu^\mu \iota \nabla^B Z_\mu.$$

The scalar product of the gradient with face vector $\iota f^\nu = \langle \iota f, {}_\nu u \rangle$, $\nu \in \{0, 1, 2\}$ is thus

$$(18) \quad \iota S = \iota f \cdot \iota \nabla Z = \underbrace{\iota f^\nu \gamma_\nu^\mu}_{=: \iota s^\mu} \iota \nabla^B Z_\mu = \iota s^\mu \iota \nabla^B Z_\mu.$$

Continuity of the gradient at cell interfaces yields linear updating equations for Z^p on the two adjacent faces. In fact, for any two neighbouring cells ζ , χ with common face, labelled ι in cell ζ and κ in χ , continuity requires

$$(19) \quad \iota S = - \kappa S.$$

Substituting (18) for ιS and κS and observing the time shifts in (13) provides the updating relations for Z^p at the cell interfaces.

To derive these explicitly, we first introduce the following quantities $\iota z_\mu^{p,n}$, ($\iota = 0, \dots, 5$; $\mu = 0, 1, 2$)

$$(20) \quad \iota z_\mu^n(t) := \begin{cases} 2(-1)^\iota Z^n|_t & \text{if } \mu = [\iota/2] \\ ({}_{2\mu+1}Z^p - {}_{2\mu}Z^p)|_{t-\tau/2} & \text{else} \end{cases},$$

which in virtue of (1) yields $\iota z_\mu^p = (p, Z) = (p^\sim, Z \circ \iota \sigma^{-1}) = \iota z_\mu^n | Z \circ \iota \sigma^{-1}$, where $\iota \sigma : n \mapsto p$ denotes the nodal shift pertinent to face ι . In particular

$$(21) \quad \iota z_{[\iota/2]}^p(t) = 2(-1)^\iota \iota Z^p|_t,$$

which together with (20) for $\mu \neq [\iota/2]$ is consistent with

$$(22) \quad \iota z_\mu^n(t + \tau/2) = -\frac{1}{2}({}_{2\mu+1}z_\mu^p + {}_{2\mu}z_\mu^p)(t).$$

From (13, 18, 20, 21) follows that

$$(23) \quad \begin{aligned} {}_{\iota}S|_{t+\tau} &= {}_{\iota}S^{\mu}({}_{\iota}z_{\mu}^n|_{t+\tau/2} - 2(-1)^{\iota}\delta_{\mu}^{[\iota/2]}{}_{\iota}Z^p|_{t+\tau}) \\ &= {}_{\iota}S^{\mu}({}_{\iota}z_{\mu}^n|_{t+\tau/2} - \delta_{\mu}^{[\iota/2]}{}_{\iota}z_{\mu}^p|_{t+\tau}) \quad . \end{aligned}$$

This, with (19,20) and the continuity of Z , i.e. ${}_{\iota}Z^p = {}_{\kappa}Z^p$, implies

$$(24) \quad {}_{\iota}z_{[\iota/2]}^p(t+\tau) = \frac{{}_{\iota}S^{\mu}{}_{\iota}z_{\mu}^n(t+\tau/2) + {}_{\kappa}S^{\nu}{}_{\kappa}z_{\nu}^n(t+\tau/2)}{{}_{\iota}S^{[\iota/2]} + (-1)^{\iota+\kappa}{}_{\kappa}S^{[\kappa/2]}} ,$$

and for completeness we agree upon setting ${}_{\iota}z_{\mu}^p(t+\tau) := {}_{\iota}z_{\mu}^n(t+\tau/2)$, for $\mu \neq [\iota/2]$. Note that the latter relations contain a slight inconsistency, in that continuity might be infringed - which is yet circumvented by taking the arithmetic means of the two adjacent values. In fact, our agreement doesn't do harm, since any discontinuity disappears with mesh refinement.

We have thus defined complete recurrence relations for z^p (given z^n on the former reflection step), which at the same time determine on face ι the field components and their gradients

$$(25) \quad {}_{\iota}\nabla Z_{\nu} = \gamma_{\nu}^{\mu}{}_{\iota}z_{\mu}^p,$$

and which essentially constitute the connection step of the algorithm. Nodal gradients are similarly, yet more simply, derived using

$$\nabla^B Z_{\mu}^n(t + \frac{\tau}{2}) := ({}_{2\mu+1}Z^p - {}_{2\mu}Z^p)(t); \quad \mu = 0, 1, 2$$

in the place of (13) and then again (17). With the node and cell-boundary values and gradients of T and \mathbf{u} , the nodal updating relations for these quantities are directly derived from equations (10, 11) in sect. 3. For equations (10) (without the convective term) this has essentially been carried out in [He1], sect. 5, and the procedure remains straightforward.

The obtained updating relations are explicit and consistent with near-field interaction (only adjacent quantities enter). So, they can optionally be transformed into scattering relations for incident and reflected quantities (3) along the guidelines of section 2 - with known advantages known for the stability estimates [He2].

5. Pressure

Pressure is a known subject sui generis in Computational Fluid Dynamics [ATP][MeSt][GDN] yet insofar as pressure fluctuations in general do not match the typical time scales of heat propagation and fluid flow. Pressure fluctuations are related to acoustic waves, the net effect of which can be important and usually has a strong impact on computational stability [LeVeque].

Pressure fluctuations also play a key role in the following procedure, which is known as *divergence cleaning* in Magnetohydrodynamics [ibid., p. 128] and ensures mass conservation in the present context.

For Boussinesq-incompressible flow, conservation of mass simply requires divergence-free flow, $\text{div } \mathbf{u} = 0$, i.e. in integral form, using Gauss' theorem, $0 = \int_{\zeta} \text{div } \mathbf{u} \, dV = \int_{\partial\zeta} \mathbf{u} \cdot dF$. Since equations (7, 8) in section 3 do not a priori ensure this, additional arrangements must be made - by means of pressure.

In a successive overrelaxation (SOR) routine, interposed between the connection and reflection steps of the iteration cycle, firstly the (discrete) right-hand side integrals $I_{\partial\zeta} = \int_{\partial\zeta} \mathbf{u} \cdot dF$ are computed, and then the pressure p which compensates $I_{\partial\zeta}$ so that

$$(26) \quad \frac{\tau}{\varrho_{\infty}} \int_{\partial\zeta} \text{grad } p \cdot dF = \int_{\partial\zeta} \mathbf{u} \cdot dF.$$

Indeed, taking for Z in the preceeding section the pressure, it follows from (20, 22) that equations (26) (in discrete form with sums over the cell faces, of course) yield a unique solution $p^n = Z^n$ for every cell, given the right-hand side integral $I_{\partial\zeta}$. Note that we are actually solving Poisson's equation $\Delta p = (\varrho_{\infty}/\tau) \text{div } \mathbf{u}$ in integral form.

With the new face pressure gradient, extracted from (20, 24, 25), the face values of \mathbf{u} are updated as $\mathbf{u} - (\tau/\varrho_{\infty}) \text{grad } p$.

After each SOR cycle, continuity of $\text{grad } p$ at the cell faces must be re-established using (19), i.e. by updating the port values of p according to (23). The chain of processes is reiterated until $\sum_{\zeta} I_{\partial\zeta} < \epsilon$ for a suitable bound ϵ (which happens after a few iterations for appropriate choices).

6. Coaxial line

To illustrate the approach in a stalwart application, we display the results of simulations with coaxial line RL240-100 under high power operating conditions (realistically inferred from a ion cyclotron resonance heating *ICRH* experiment in plasma physics).

The inner and outer conductors of diameters 100 mm and 240 mm are made of copper and aluminium, respectively, and the rigid line is filled with air at atmospheric pressure. We have simulated the heating process from standby to CW operation at frequency 100 MHz and 160 kW transmitted power for horizontal position of the line and with outer conductor cooled at 40 degrees Celsius fixed temperature.

Figure 4 b displays the air flow profile (vertical section) computed for the transient state one minute after switch-on. The natural convection pattern is clearly visible and nicely developed.

The computations have been carried through with a 3D-mesh of 10 layers in axial direction, over 200 millimeters of line, the transverse cross section of which is displayed in figure 4 a. At the metallic interfaces no-slip boundary conditions are implemented and free-slip conditions at all other boundaries.

Simultaneously, a Maxwell field TLM algorithm was run to provide the heat sources.

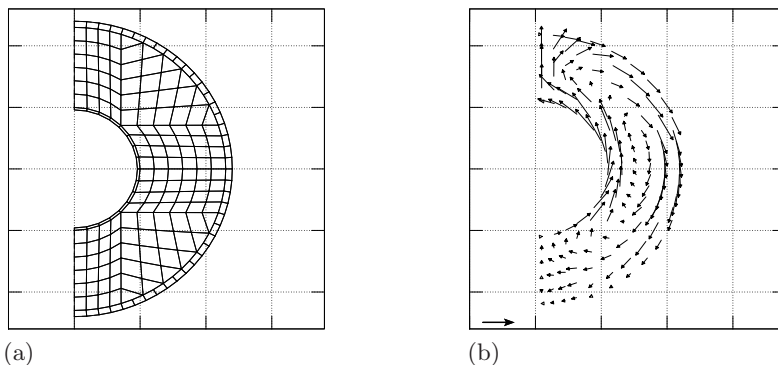


Fig. 4. (a) mesh (b) velocity profile [reference arrow: 2 cm/s]

7. Conclusions

A prototypical implementation of the OBERBECK-BOUSSINESQ approximation to viscous flow has been presented in this paper, which demonstrates the fundamental fitness of the DSC approach for fluid dynamic applications. In this respect, at least (that was recently called into question by a TLM expert), DSC schemes significantly transcend the range of application of the TLM method, from which they descend.

A next natural step in the line of this study is of course the implementation of turbulence models which are compatible with the Boussinesq approach, such as the $k - \epsilon$ model [ATP], first of all. - We hope this paper stimulates some interest into joint further investigation in that direction.

References

- [MeSt] Meister, A., Struckmeier, J., *Hyperbolic Partial Differential Equations* Theory, Numerics and Applications, Friedrich Vieweg and Sohn, Göttingen 2002
- [LeVeque] LeVeque, R.J., Mihalas, D., Dorfi, E.A., Müller, E. *Computational Methods for Astrophysical Fluid Flow*, Saas Fee Advanced Courses, 27, Springer-Verlag Berlin Heidelberg, 1998
- [GDN] Griebel, M., Dornseifer, T., Neunhoffer, T., *Numerical Simulation in Fluid Dynamics*, SIAM monographs on mathematical modeling and computation, Society for Industrial and Applied Mathematics, 1998
- [ATP] Anderson, D.A., Tannehill, J.C., Pletcher, R.H., *Computational Fluid Mechanics and Heat Transfer*, series in computational methods in mechanics and thermal sciences, Hemisphere Publishing Corporation, 1984
- [Bss] Boussinesq, J., *Théorie Analytique de la Chaleur*, Gauthiers-Villars, 2., Paris 1903

- [Ch] Christopoulos, C., *The Transmission-Line Modeling Method TLM*, IEEE Press, New York 1995
- [dCo] De Cogan, D., *Transmission Line Matrix (TLM) Techniques for Diffusion Applications*, Gordon and Breach, 1998
- [Obb] Oberbeck, A., Über die Wärmeleitung der Flüssigkeiten bei Berücksichtigung der Strömung infolge Temperaturdifferenzen., Ann. Phys. Chem., vol. 7, pp. 271-292, 1879
- [JoB] Johns, P.B., Beurle R.L., Numerical solution of 2-dimensional scattering problems using transmission line matrix, Proc. IEEE, vol. 118, pp. 1203-1208, 1971
- [Jo1] Akhtarzad, S., Johns, P.B., Solution of 6-components electromagnetic fields in three dimensions and time by the T.L.M. method, Electron. Lett. vol. 10, pp. 535-537, Dec. 12, 1974
- [Jo2] Johns, P.B., A symmetrical Condensed Node for the TLM Method, IEEE Trans. Microwave Theory Tech., vol. 35, pp. 370-377, April 1987
- [Jo3] Johns, P.B., A simple, explicit and unconditionally stable numerical routine for the solution of the diffusion equations, Int. J. Numer. Methods Eng., vol. 11, pp. 1307-1328, 1977
- [Tlm1] Proceedings of the 1st Int. Workshop on Transmission Line Matrix (TLM) Modelling, Victoria, 1995
- [Tlm2] Proceedings of the 2nd Int. Workshop on Transmission Line Matrix (TLM) Modelling, TU München, 1997
- [Tlm3] Proceedings of the 3rd Int. Workshop on Transmission Line Matrix (TLM) Modelling, Université de Nice, 1999
- [Re] Rebel, J.N., On the Foundations of the Transmission Line Matrix Method, Thesis, TU München, 2000
- [Hf1] Hoefer, W. J. R., The Transmission Line Matrix (TLM) Method, in Numerical Techniques for Microwave and Millimeter-Wave Passive Structures, T. Itoh ed., John Wiley & Sons, 1989
- [He1] Hein, S., Dual scattering channel schemes extending the JOHNS Algorithm, submitted for publication
- [He2] Hein, S., On the stability of dual scattering channel schemes, <http://arxiv.org/abs/math.NA/0405095>, preprint, May 2004
- [He3] Hein, S., Finite-difference time-domain approximation of Maxwell's equations with nonorthogonal condensed TLM mesh, Int. J. Num. Modelling, vol. 7, pp. 179-188, 1994
- [He4] Hein, S., Gauge techniques in time and frequency domain TLM, Computer Physics Communications, vol. 136, pp. 77-89, 2001
- [He5] Hein, S., Synthesis of TLM Algorithms in the Propagator Integral Framework, Proceedings of the 2nd. Int. Workshop on Transmission Line Matrix Modeling (TLM) - Theory and Applications, pp. 1-11, München, October 1997 (invited paper)
- [He6] Hein, S., TLM numerical solution of Bloch's equations for magnetized gyrotropic media, Appl. Math. Modelling, vol. 21, pp. 221-229, 1997
- [He7] Hein, S., A TLM node for superconducting boundary illustrating the propagator approach, Spinner Report E017, München 1992
- [He8] Hein, S., Consistent finite difference modelling of Maxwell's equations with lossy symmetrical condensed TLM node, Int. J. Num. Modelling, vol. 6, pp. 207-220, 1993

SPINNER GmbH. München; Aiblinger Str. 30, DE-83620 Westerham
 E-mail address: s.hein@spinner.de